METRICA
METRology Institutional CAtalog

ISTITUTO NAZIONALE DI RICERCA METROLOGICA
Repository Istituzionale

Performance assessment methods and metrics for passive daytime radiative cooling materials

Original
Performance assessment methods and metrics for passive daytime radiative cooling materials / Werle, J., Tichý, D., Efthymiou, C., Assimakopoulos, M., Voldán, M., Pattelli, L.. - In: CELL REPORTS PHYSICAL SCIENCE. - ISSN 2666-3864. - 7:4(2026). [10.1016/j.xcrp.2026.103225]

Availability:
This version is available at: 11696/89399 since: 2026-03-31T21:25:38Z

Publisher:
Elsevier

Published
DOI:10.1016/j.xcrp.2026.103225

Terms of use:

This article is made available under terms and conditions as specified in the corresponding bibliographic description in the repository

Publisher copyright

(Article begins on next page)

09 June 2026

Please cite this article in press as: Werlé et al., Performance assessment methods and metrics for passive daytime radiative cooling materials, Cell Reports Physical Science (2026), https://doi.org/10.1016/j.xcrp.2026.103225

Cell Reports
Physical Science

CellPress
OPEN ACCESS

Perspective

Performance assessment methods and metrics for passive daytime radiative cooling materials

Jérémy Werlé,[1] David Tichý,[2,4] Chrysanthi Efthymiou,[3] Margarita-Niki Assimakopoulos,[3] Michal Voldán,[2] and Lorenzo Pattelli[1,*]

[1]Istituto Nazionale di Ricerca Metrologica (INRiM), 10135 Turin, Italy
[2]Czech Metrology Institute, Regional Branch Praha, 10200 Prague, Czech Republic
[3]National and Kapodistrian University of Athens, 10559 Athens, Greece
[4]Present address: Department of Chemical Engineering, University of Chemistry and Technology Prague, Prague 16628, Czech Republic
*Correspondence: l.pattelli@inrim.it
https://doi.org/10.1016/j.xcrp.2026.103225

SUMMARY

Passive daytime radiative cooling (PDRC) is an emerging, electricity-free cooling approach that can achieve sub-ambient temperatures by emitting thermal radiation through the atmospheric transparency window (8–13 μm). It therefore offers a promising route to mitigate the growing demand for cooling across a broad range of applications. As the number of reported PDRC materials and demonstrations increases rapidly, robust and broadly comparable figures of merit (FoMs) and testing protocols are increasingly needed to assess performance and to translate laboratory results to diverse outdoor conditions. However, commonly used FoMs and experimental methods are often reported inadequately or without key experimental information, which hampers reproducible benchmarking and cross-study comparison. This perspective critically reviews the main classes of spectral and thermally derived FoMs. In doing so, it discusses numerical and experimental testing approaches by highlighting recurring limitations that drive discrepancies between studies. Building on this analysis, we propose a metrological framework for the classification and comparison of PDRC materials and provide a minimum reporting checklist to enable efficient inter-laboratory comparison and more reliable performance assessment.

INTRODUCTION

The past 11 years have been the 11 warmest since the beginning of meteorological records, with 2024 certified as the first to exceed 1.5°C above pre-industrial levels.[1] The expansion of urban areas, coupled with the heat island effect, further increases the cooling demand, which is projected to triple by 2050.[2] The anticipated rise in electricity consumption poses an urgent need to explore new cooling strategies and technologies. Passive radiative cooling (PRC) leverages spontaneous heat radiation in the long-wave infrared (IR) transparency window of the atmosphere (8–13 μm), potentially enabling cooling below ambient temperature without external energy input.[3,4] This process has the potential to reduce cooling energy demand and mitigate the urban heat island effect without greenhouse gas emissions, unlike traditional mechanical vapor compression coolers.[5] Due to its working principle, unobstructed access to a clear sky and strong emissivity in the 8–13 μm wavelength range are essential for effective passive daytime radiative cooling (PDRC) performance. During the day, strong solar irradiance makes it particularly challenging to achieve PDRC. However, significant progress was made in the past decade, thanks to the development of advanced manufacturing techniques[5] required to tune the spectral response of such materials across the whole solar spectrum (0.3–3 μm) while maintaining high emissivity with the sky transparency window. This advancement has led to the development of numerous innovative PDRC material designs[6,7] and full-scale cooling system architectures.[8,9] Despite this progress, however, the field still faces notable challenges. In particular, the use of inconsistent performance evaluation methods, along with incomplete or inaccurate reporting of key figures of merit (FoMs), hinders a comprehensive and reliable assessment of the current state of the art of this technology.[10] Recognizing and overcoming these challenges is essential for driving further improvement and facilitating the broader adoption of PDRC in real-world applications. This perspective aims to identify key FoMs for PDRC materials, thereby contributing to a more consistent framework for defining and evaluating the potential of this emerging technology.

Spectral and spectrally derived FoMs

The spectral response of a PDRC material is arguably the most important characteristic that determines its cooling potential. Accurate evaluation of this property lies at the core of any performance assessment. In principle, emissivity across the full wavelength range can be measured directly by comparing the thermal

This is an open access article under the CC BY license (http://creativecommons.org/licenses/by/4.0/).

Please cite this article in press as: Werlé et al., Performance assessment methods and metrics for passive daytime radiative cooling materials, Cell Reports Physical Science (2026), https://doi.org/10.1016/j.xcrp.2026.103225

radiation emitted by a sample to that of calibrated blackbodies at a controlled temperature.[10,11] These measurements can be used to provide highly accurate directional and hemispherical spectral data but require specialized instrumentation, careful temperature control, and often multiple measurement setups for the solar and IR ranges.

More commonly, emissivity is inferred indirectly via absorptivity using Kirchhoff's law (i.e., $\epsilon(\lambda,\theta) = a(\lambda,\theta)$). Absorptivity is computed as $a(\lambda,\theta) = 1 - t(\lambda,\theta) - r(\lambda,\theta)$, where r and t are the directional-hemispherical reflectance and transmittance measured via integrating-sphere spectrophotometry.[7,11] In this perspective, the discussion is limited to opaque, UV-Vis-NIR reflective PDRC coatings and solid reflectors, which represent the dominant class of PDRC materials. Semi-transparent coatings (e.g., for agricultural or smart-window applications) and textile-based systems raise additional characterization requirements (e.g., transmittance, breathability/wicking, and thermal-contact control) and are outside the present scope. For this class of materials, the first common issue in the literature is that true hemispherical emissivity is rarely measured, and near-normal values are often reported instead. Because ϵ generally decreases at high angles for opaque emitters, approximating directional emissivity by normal values tends to overestimate RC potential and weakens the correlation between reported optical FoMs and actual performance.[12] Standardized extrapolation methods exist to estimate hemispherical emissivity (e.g., DIN EN 410, ISO 9050, and ASTM E1585-93), but their validity for heterogeneous or nanostructured PDRC materials remains largely untested. Directional-hemispherical measurements are therefore commonly adopted as a practical alternative, although they are not exempt from experimental limitations. Accordingly, specific experimental recommendations are required to ensure data reliability.

To ensure reliable spectral data, Bu et al.[10] recommend performing at least two independent measurements per sample. In our experience, repeating at least three scans per sample—with removal and repositioning between scans—provides a more robust estimate by reducing positioning- and alignment-related variability, enabling meaningful averaging. Moreover, for anisotropic or heterogeneous materials (e.g., industrially manufactured polymer films that may exhibit a processing direction or fibrous structures such as delignified wood), measurements in multiple in-plane orientations are essential to quantify experimental uncertainty. Additionally, many UV-Vis-NIR spectrophotometers employ different detectors across the UV-Vis and NIR ranges,[13] with a crossover typically near 800 nm. Step-like discontinuities around this crossover can arise from detector/source switching and are unfortunately common in published spectra, which can make a significant difference in the determination of spectrally integrated quantities. As a consistency check, the crossover wavelength can be shifted (e.g., by ±50 nm) and/or the reference-beam intensity adjusted in common double-beam spectrophotometers to verify spectral continuity and exclude instrumental artifacts. The accuracy of the measured spectra also relies on precise instrument calibration and absolute reflectance measurements that account for the reflectance of the reference diffuser and the integration of the sphere material's coating.[10] Inter-laboratory studies further demonstrate that variability in reported optical properties is significant among laboratories and well above nominal instrumental uncertainty, arising from variations in calibration procedures, detector configurations, and laboratory practices.[14] This observation underscores that spectral quantities should not be interpreted as exact material constants but as measured values whose uncertainty includes both instrumental and procedural contributions. For materials containing photoluminescent additives (fluorescent or phosphorescent), conventional spectrophotometric reflectance measurements can be biased because emitted light may be detected outside the monochromator setting; such systems require dedicated protocols and are not treated here.[15] Similarly, stimuli-responsive materials (e.g., phase-change, thermo/electrochromic, and switchable designs) require state-resolved, temperature-controlled spectral characterization and application-specific FoMs and are outside the present scope.

From spectral measurements, several FoMs can be derived. Two of the most common are the solar reflectance and the thermal emissivity[7,16]:

$$r_{\text{solar}} = \frac{\int_{0.3\ \mu\text{m}}^{3\ \mu\text{m}} r(\lambda,\theta=0,T) I_{\text{solar}}(\lambda)\,\mathrm{d}\lambda}{\int_{0.3\ \mu\text{m}}^{3\ \mu\text{m}} I_{\text{solar}}(\lambda)\,\mathrm{d}\lambda} \text{ and}$$

$$\epsilon_{\text{IR}} = \frac{\int_{3\ \mu\text{m}}^{30\ \mu\text{m}} \epsilon(\lambda,\theta=0,T) I_{\lambda,\text{b}}(\lambda,T)\,\mathrm{d}\lambda}{\int_{3\ \mu\text{m}}^{30\ \mu\text{m}} I_{\lambda,\text{b}}(\lambda,T)\,\mathrm{d}\lambda}, \text{ respectively,} \quad \text{(Equation 1)}$$

where $I_{\text{solar}}(\lambda)$ is the reference solar spectral irradiance used to compute the solar-weighted reflectivity, $I_{\lambda,\text{b}}$ is the blackbody spectral radiance at temperature T and wavelength λ, and $\epsilon(\lambda,\theta=0,T)$ and $r(\lambda,\theta=0,T)$ are the normal emissivity and reflectivity at a given temperature and wavelength. In a large part of the PDRC literature, $I_{\text{solar}}(\lambda)$ is often taken as AM1.5G (e.g., the ASTM G173 global spectrum tabulated by National Renewable Energy Laboratory [NREL]).[17] However, for estimating solar heat gain under typical horizontal outdoor illumination, Levinson et al.[18] recommend using the clear-sky air-mass-one global-horizontal spectrum (AM1GH) to predict solar heat gain more accurately over a wide latitude range.[18] Accordingly, we recommend reporting r_{solar} computed with both AM1.5G (for cross-study comparability) and AM1GH (for heat-gain relevance), since the additional computation is straightforward once $r(\lambda)$ is known. The combination of spectrally integrated r_{solar} and ϵ_{IR} provides intuitive visualization and allows wide material comparisons. However, their predictive value depends on the spectral integration limits and whether directional or hemispherical values are used, which can obscure differences between broadband and selective emitters. Because integration bounds vary across the literature (e.g., solar integration ending at 2.5, 3, or 4 μm or IR integration starting at 3, 5, or higher μm), the chosen wavelength ranges should always be stated explicitly to ensure comparability.

Selectivity descriptors, such as the ratio $\eta = \epsilon_{\text{sky}}/\epsilon_{\text{IR}}$,[19] quantify emission within the atmospheric window relative to the broader thermal IR. Here, ϵ_{sky} denotes the Planck-weighted emissivity integrated over the sky window (commonly 8–13 μm). Higher η values indicate stronger spectral selectivity,

Please cite this article in press as: Werlé et al., Performance assessment methods and metrics for passive daytime radiative cooling materials, Cell Reports Physical Science (2026), https://doi.org/10.1016/j.xcrp.2026.103225

but they neglect solar absorption and therefore correlate only partially with net cooling performance.

Temperature-aware metrics attempt to bridge optical measurements and real-world thermal behavior. The solar reflectance index (SRI), defined in ASTM E1980-11,[20] maps solar reflectance and broadband thermal emittance to a normalized surface-temperature scale under prescribed conditions (310 K, 1,000 W m^{-2}). The scale is anchored such that a standard black surface has SRI = 0 and a standard white surface has SRI = 100. Modern cool coatings can reach SRI > 100, indicating surfaces cooler than the white reference under the same standardized assumptions. However, the SRI is spectrally averaged and does not, by itself, guarantee sub-ambient cooling; its applicability to spectrally selective PDRC materials is therefore limited. Fabiani et al.[21] recently proposed a modified SRI* improving predictive capability by incorporating a wavelength-dependent sky temperature and hemispherical emissivity, which, however, introduces model dependence and requires detailed atmospheric and site-specific inputs. An earlier attempt to define a FoM tailored to PDRC materials was made by Li et al.,[22] with the RC metric defined as:

$$RC = \epsilon_{sky} - r(1 - r_{solar}), \quad \text{(Equation 2)}$$

where ϵ_{sky} is the emissivity in the atmospheric window, r_{solar} the solar reflectance, and r the solar-to-blackbody power ratio. The RC descriptor is simple and environment independent but cannot distinguish broadband from selective emitters or account for angular effects.

An important criterion for PDRC materials is the temporal evolution of their spectral FoMs, which reflects aging. For opaque, highly emissive materials, emissivity has been found to remain nearly constant (± 0.05),[23] whereas aging mainly degrades solar reflectance, a key factor for long-term outdoor performance. Despite its importance, natural aging results are seldom reported due to long test durations and strong dependence on climate, weather, and installation conditions.[24] In the US, the SRI of roofing products must be reported after 3 years of outdoor exposure across Phoenix, AZ; Miami, FL; and Medina, OH, to qualify for commercialization. To shorten evaluation times, ASTM D7897 describes an accelerated protocol combining UV exposure (ASTM G154) and soiling, initially developed by Sleiman et al.[25–27] and later adapted for European climates.[24] Although such protocols were not developed specifically for PDRC materials, they provide a practical starting point for accelerated durability screening. At the same time, they may not capture specific effects such as biological growth or condensation-driven soiling, which can be more relevant for PDRC surfaces.

In summary, spectral FoMs span multiple objectives, from rigorous absolute measurements[10,11] to compact scalar indicators for rapid comparison (η, RC, and SRI*; see also Table S1). For reproducible, physically meaningful assessment of PDRC materials, integrated solar reflectance and IR emissivity should be reported together with the measurement geometry (directional vs. hemispherical) and the adopted spectral integration limits. While near-normal values can overestimate hemispherical emissivity for opaque samples, they are accessible and reproducible and provide a useful baseline for comparison when reported transparently. Whenever possible, spectral-directional (angle-resolved) emissivity—or at least directional emissivity integrated over the sky window—is additionally required for non-horizontal installations (e.g., vertical radiative coolers), where upward/downward emissivity asymmetry can mitigate parasitic radiation exchange with the ground.[28]

That said, optical spectra alone are not exhaustive descriptors of RC performance: materials with similar optical properties may still exhibit different thermal behavior due to thermophysical properties and parasitic heat-transfer pathways. Thermal characterization (outdoor or controlled) therefore remains an important complement to spectral FoMs for establishing performance benchmarks and enabling meaningful cross-laboratory comparisons.[7,10]

Thermally derived FoMs

The choice of thermal metric and experimental protocol strongly depends on the purpose of the test. Performance-oriented tests aim to quantify the intrinsic maximum capabilities of the material under nearly ideal conditions, minimizing parasitic heat fluxes from the environment. In contrast, application-oriented tests seek to reproduce real-world operating conditions, for instance by simulating surface temperatures of buildings and other thermal masses, cold-water cooling, or other practical implementations. Within this perspective, the focus will be given to performance-oriented FoMs to provide more general guidelines to access maximum performances without enumerating specific test applications.

The two classical FoMs used to thermally characterize PDRC materials are the maximum sub-ambient temperature drop (ΔT_{max}) obtained at vanishing net cooling power (Figure 1A) and the net cooling power (P_{net}) of PDRC materials (see Note S1), which is either reported experimentally with the sample kept at ambient temperature or inferred numerically.

In their seminal demonstration, Raman et al.[4] proposed an experimental method using an external electric heating pad applied under the sample, allowing for the determination of P_{net} as the electric power required to maintain the sample at ambient temperature, controlled via a feedback loop (Figure 1B).

This approach operates at ambient temperature, thus eliminating convective contributions, but it assumes that all heater-generated heat is transferred to the sample and dissipated through its surface. Any deviation, such as lateral heat losses or insufficient thermal insulation, can lead to overestimation. Advanced heating systems with thermal guarding, as applied by Leroy et al.,[29] can mitigate these errors. Alternatively, a more advanced heat-flow sensor can be used to directly measure the cooling power instead of relying on electrical-to-power conversion.[30]

An alternative method leverages a heat-transfer fluid in contact with the emitter's backside or flowing inside the emitter's substrate (Figure 1C). In this configuration, P_{net} is calculated as

$$P_{net} = \dot{m}_{fluid} c_p \Delta T / A, \quad \text{(Equation 3)}$$

where $\dot{m}_{fluid}$ is the fluid mass flow rate, c_p its specific heat, ΔT the inlet-outlet temperature difference, and A the sample area. This method ensures highly reproducible thermal contact and accurate measurement of temperatures and flow rates, providing

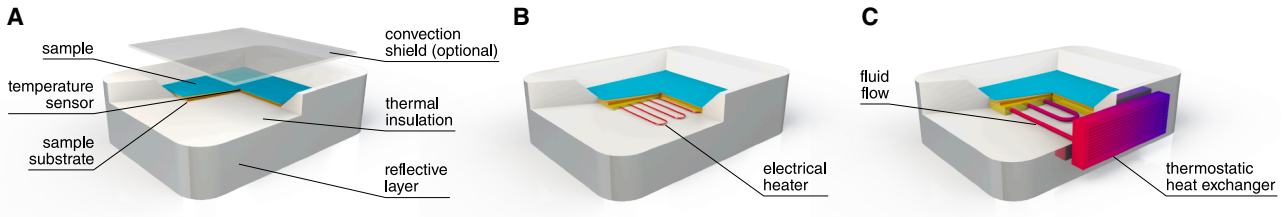

Figure 1. PDRC outdoor test configurations used for temperature-drop and cooling power reporting

(A) Sample holder thermally insulated with thick polystyrene foam and protected from solar radiation by a suitable reflective layer to minimize solar gains. The sample cavity may optionally be covered with an IR-transparent barrier to reduce convection or with more advanced cover layers that offer higher solar reflectivity or mechanical resistance when needed (e.g., for depressurized enclosures).

(B) System incorporating an electric heater or heating pad controlled via feedback loop. The measured cooling power corresponds to the electrical power consumed by the heating element.

(C) System using a flowing fluid (e.g., water) that is cooled down by the PDRC material, enabling the evaluation of cooling power through the known flow rate and measured temperature drop.

precise cooling power determination. Additionally, compared to the electric heating method, it allows, in principle, measurement of both negative and positive heat fluxes, depending on the temperature set point of the heat-exchange fluid. On the downside, in order to generate measurable temperature differences, large panel areas or slow flow rates are typically required, which introduce significant thermal inertia and temperature gradients across the exposed surface, thus amplifying non-radiative parasitics.[31] More recent metrology-driven implementations have shown that these limitations can be substantially mitigated through optimized flow-channel design and the use of multi-junction differential thermopiles, enabling SI-traceable temperature-difference measurements with expanded uncertainties on the order of ≈10 mK and relative cooling-power uncertainties below 10% across most of the PDRC-relevant flux range.[32] These developments illustrate that the attainable accuracy of fluid calorimetry depends not only on geometry and flow rate but also critically on sensor architecture and full uncertainty budgeting.

Although thermal FoMs are simple to define, accurately determining them is challenging because they depend strongly on both environmental conditions and test configuration. Atmospheric transparency affects radiative exchange and is highly sensitive to humidity, as water vapor absorbs in the 8–13 μm band, making high cooling performance more difficult to achieve in humid regions.[33] Because humidity also depends on altitude, the testing site elevation is also a relevant factor. Local aerosol loading can further reduce IR transparency,[3] while the angular dependence of sky emissivity makes sample orientation and incidence angle important.[19,34,35] The test site surrounding the environment also matters: a reduced view factor of the sky (e.g., due to nearby buildings or vegetation) limits achievable cooling.[36]

In addition to radiative exchange, non-radiative heat transfer can affect the measured FoMs. Both natural (buoyancy-driven) and forced (wind-driven) convection are typically lumped into an effective heat-transfer coefficient, often modeled empirically as a constant term plus a wind-speed-dependent contribution.[37] Because reported coefficients vary substantially across studies, reporting wind speed and setup geometry is essential, and estimating the effective non-radiative coefficient for a given configuration is highly valuable, for instance, via paired rigs that measure both temperature drop and cooling power under matched conditions[38] or by taking advantage of transient relaxation to ambient conditions using pre-cooled thermal masses.[39] Because sub-ambient performance is defined relative to the ambient air temperature, the definition and measurement of ambient temperature critically affect reported ΔT_{max} and P_{net} values. Improperly shielded sensors or enclosed air pockets can bias the reference temperature and inflate apparent cooling.[13,40] Ambient temperature should therefore be measured outside the holder, in a properly ventilated radiation shield (e.g., a Stevenson screen), and the sensor type, placement, and calibration/uncertainty should be reported.

Comprehensive evaluation benefits from reporting both the maximum net cooling power, $P_{net,max}$, and the maximum temperature drop, ΔT_{max}, under matched environmental conditions, ideally measured simultaneously.[41] Concurrent measurements help reduce weather-driven bias and can be used to infer non-radiative losses and other parasitic contributions.[38] Side-by-side measurements on multiple samples further improve comparability and can reveal differences driven by thermophysical factors even when optical spectra are similar. Benchmarking against reproducible reference materials, such as do-it-yourself (DIY) silver-mirror/selective Scotch tape devices or industrially manufactured samples, is key for improving comparability across studies.[11,42,43]

Despite these challenges, outdoor testing remains the most application-relevant approach for assessing PDRC performance (see Table S2) and should be complemented by optical FoMs to ensure internal consistency. Careful monitoring and reporting of key environmental parameters—including humidity, wind speed, solar irradiance, downwelling long-wave radiation (or equivalent sky temperature), and local sky view factor—is essential for enabling inter-laboratory comparisons. Given the strong dependence of thermal FoMs on location and climate, coupling thermal measurements with spectral FoM analysis and numerical simulations can help verify data consistency and relativize the influence of local boundary conditions on reported performance. In addition, the design of the outdoor experimental setup plays a critical role, as discussed in the following section.

Please cite this article in press as: Werlé et al., Performance assessment methods and metrics for passive daytime radiative cooling materials, Cell Reports Physical Science (2026), https://doi.org/10.1016/j.xcrp.2026.103225

CellPress
OPEN ACCESS

FoMs for outdoor setup construction

The experimental setup for assessing maximum performance must be carefully designed to minimize environmental artifacts. Its primary objective is to suppress parasitic conductive heat transfer and to limit unwanted heat gains from solar irradiation, wind-driven convection, and long-wave IR radiation from surrounding surfaces.[4,29] In most reported setups, the sample is mounted on a thick expanded polystyrene (EPS) base that provides thermal insulation. The insulation material should be covered on its outer surfaces with a reflective layer to reduce solar heating of the holder and to protect it from rapid degradation under prolonged solar UV exposure. At the same time, however, direct contact between a reflective shield and the sample can introduce parasitic conduction and should be avoided. Different design strategies are often required for the sky-facing surface and for the lateral walls of the holder. Lateral walls usually have a low sky view factor and are more exposed to long-wave radiation from the ground and nearby objects. Multilayer sidewalls that combine reflective foils, air gaps, and additional insulation can therefore reduce lateral heat fluxes. While Hu et al.[44] suggest an insulation foam thickness of at least 10 cm, a more conservative thickness of 20 cm is often needed to limit conductive contributions to $\leq$1 W m^{-2}.[16] Beyond insulation thickness, the radiative behavior of sky-facing holder surfaces can also bias measurements. Any sky-facing area not covered by the test sample should ideally remain close to ambient temperature to avoid perturbing the local air temperature and the long-wave exchange with the sample. For sufficiently large samples, this can be achieved by extending the PDRC material over the full top surface of the insulating base. For smaller samples, aluminum-backed spunbonded polyethylene (PE)-fiber sheets (e.g., Tyvek) or, when practical, the PDRC material itself can be used to cover the remaining sky-facing area. Such coverings provide high solar reflectivity while maintaining low broadband emissivity, helping keep the surrounding air near ambient temperature and reducing holder-induced artifacts, especially compared to commonly used alternatives such as aluminized Mylar, which can heat substantially under direct sunlight.

To quantify parasitic heat losses from the sample holder, Catalanotti et al.[39] proposed a practical method, which can be used to determine the effective heat transfer coefficient B and the box equivalent heat capacity X. A body of known heat capacity C (e.g., a pre-cooled metal plate) is placed in the holder and its temperature $T(t)$ is recorded as it relaxes toward its equilibrium temperature T_∞. Repeating the measurement for multiple C values yields decay curves that follow

$$(C + X)\frac{dT}{dt} = -B(T - T_\infty). \quad \text{(Equation 4)}$$

Fitting these curves allows estimation of B (in W K^{-1}), accounting for conduction, natural convection, and radiative losses, and X, which captures the holder's thermal inertia. These parameters can then correct PDRC measurements to ensure accurate evaluation of the sample's net cooling power, while repeated trials provide an estimate of experimental uncertainty.

In the literature, convection is often reduced by adding an IR-transparent PE film above the sample, which can act as a mechanical wind barrier while remaining largely transparent in the solar and sky-window bands. In practice, however, fully wrapping the holder in PE can create a stagnant air pocket that warms above ambient during daytime (and cools at night), leading to biased estimates of ΔT_{max} and P_{net}. For this reason, if a PE shield is used, the cavity temperature should be monitored, and the ambient reference temperature must be measured outside the enclosure in a properly ventilated radiation shield (e.g., a Stevenson screen).[45,46] The PE film should also be optically characterized, as it can reduce solar transmittance by roughly 10% and may introduce wavelength-dependent attenuation. If wind protection is necessary, we recommend using lateral PE walls or windbreaks surrounding the setup without blocking free air circulation because they reduce forced convection without introducing a greenhouse-like enclosure.[41]

At the sample level, good thermal contact and efficient heat conduction between the heating element and the sample (in heater-controlled setups) or between the flowing fluid and the sample (in flowing-fluid configurations) are essential to ensure that heat is primarily transferred into the sample rather than dissipated to other elements such as the surrounding air or the sample holder. Without this condition, the assumption of one-dimensional heat flow between the heater and the sample would no longer be valid, and additional corrections would be required. At the same time, the thermal load should remain relatively small so as not to significantly perturb the system dynamics. Furthermore, not all PDRC materials are self-standing; for example, paint samples require a supporting substrate. The choice of substrate material directly affects the sample's thermal inertia and measured performance, particularly with respect to cooling power. For this reason, a high-thermal-conductivity metal substrate, such as copper or aluminum, with a thickness of $\leq$1 mm, is generally preferred. Given its favorable balance between thermal conductivity, cost, and availability, aluminum is a convenient and common choice for the substrate material.

At the local scale, accurate determination of the temperature difference between the sample and the ambient air critically depends on the choice of temperature sensors. K-type thermocouples or platinum resistance thermometers are preferred due to their nearly linear response over the relevant temperature range, in contrast to negative temperature coefficient (NTC) thermistors, unless they undergo prior calibration or have their associated measurement uncertainty explicitly quantified.[16,41]

Beyond sample holder design and sensor selection, reliable outdoor testing also requires careful consideration of test duration and environmental conditions. While Wang et al.[16] recommend a 24-h experiment, we suggest extending the test to at least 1 full week under favorable weather. This longer duration allows for capturing general trends and averaging maximum temperature drops and cooling power rather than relying on instantaneous peak values. Additionally, initial measurements may differ significantly from subsequent days due to dew accumulation on the cooling surface. On the first day, dew is typically absent when the experiment starts in the morning, but on the following days, the sample may cool below ambient temperature and reach the dew point during early morning hours under clear skies. These dew-related effects, often associated with typical hallmarks in the temperature and cooling power profiles, provide

important data that should be analyzed alongside the standard performance metrics.

Furthermore, to facilitate inter-laboratory comparisons of thermal FoMs, tests should be performed during periods that include at least 2 days of clear-sky conditions with high solar irradiance—typically summer in the Northern Hemisphere and winter in the Southern Hemisphere—and under no-wind or low-wind conditions. Although this restricts the testing window, it provides more consistent and conservative conditions for reliable PDRC performance assessment. During these periods, the sun is relatively high in the sky, reducing the need for custom tilting of the sample to achieve adequate solar flux. A typical peak solar irradiance reaching the sample under such conditions ranges between 800 and 1,000 W m^{-2}.

Overall, the setup must carefully balance solar shielding, IR transparency, convective control, and minimal conductive pathways to ensure that the measured ΔT_{max} and $P_{net\ max}$ accurately reflect the radiative performance of the material rather than artifacts of the apparatus[4,11,29,41] (more details see Tables S2 and S5).

Numerical methods

Fully numerical approaches are an essential complement to experimental characterization for assessing PDRC performance and extrapolating it across climates and system scales. Modeling frameworks span multiple levels of complexity, ranging from full-wave electromagnetic solvers (e.g., finite-difference time-domain, finite element method, and rigorous coupled-wave analysis) computing spectral reflectance, transmittance, and emissivity from material geometry and optical constants[47] to energy-balance models that couple these spectral properties with atmospheric and climatic inputs[33,48,49] (see Table S3). While electromagnetic simulations provide a rigorous foundation for optical design, they do not directly yield cooling performance unless coupled to thermal or environmental models.

As mentioned in the previous sections, atmospheric emissivity, and in particular the effective aperture of the sky transparency window, is highly sensitive to humidity, gas composition, and cloud properties. In practice, the quantity of direct relevance for PDRC energy-balance calculations is the downwelling longwave sky irradiance (spectral or band averaged). However, intermediate descriptors such as sky emissivity and ''effective sky temperature'' are often used to approximate it. In this context, simplified empirical correlations linking sky emissivity or temperature to ambient conditions (relative humidity, temperature, and cloud fraction) are often adopted,[50] but their validity is climate dependent and often requires local calibration. Another widely used shortcut starts from the atmospheric transmittance of standard atmospheric profiles to reconstruct sky emission using Kirchhoff-type arguments (often combined with cosine scaling to recover angular dependence). Such transmittance-based reconstructions can be biased in a thermally stratified atmosphere, as absorption of gas species at high altitude does not translate into strong downwelling emission.[51]

More rigorously, the downwelling atmospheric irradiance should be computed directly using radiative transfer tools such as MODTRAN[52] or the Planetary Spectrum Generator (PSG),[53] driven by reanalysis datasets (e.g., MERRA-2 or ERA5) or typical meteorological year databases.[33,48,54] These models enable global or regional performance mapping under idealized broadband or selective-emitter assumptions,[33] as well as time-resolved simulations for specific locations.[49]

Within this critical atmospheric modeling step, cloud representation remains a major source of uncertainty: some approaches incorporate clouds through empirical attenuation factors or cloud-temperature assumptions,[33,55] while others rely on cloud-base-height-dependent formulations to estimate cloud temperature and radiative impact.[56] Accurate treatment of cloudy conditions generally requires either long-term statistical analyses or explicit cloud parameters, such as cloud base height and coverage, to estimate an effective cloud view factor.[57] Recent radiative transfer schemes based on ERA5 states and the use of RRTM_LW can provide time- and site-specific band-averaged downwelling longwave irradiance, even though angular resolution is still lacking.[54]

At the system and building scales, PDRC models are increasingly embedded within building energy simulation frameworks to evaluate cooling power, energy savings, and interactions with heating, ventilation, and air conditioning (HVAC) systems.[55,58,59] While these approaches improve practical relevance, they often rely on strong assumptions regarding building archetypes, cloud handling, and material angular emissivity. Numerical optimization studies further exploit these models to generate statistically representative performance metrics, either by decoupling material radiative properties from environmental variability using daily-averaged conditions[30] or by condensing year-long performance into accumulated cold-energy metrics.[57] These simplifications improve computational tractability but may obscure transient effects and extreme conditions.

To make simulations interpretable and reusable, studies should report the full set of inputs, material spectra and geometry, boundary conditions, and numerical settings, as well as the provenance of atmospheric and meteorological data. When possible, providing openly accessible code, scripts, or input data facilitates verification and benchmarking across research groups. Numerical predictions should be interpreted alongside experimentally validated spectral data and, whenever feasible, cross-checked against thermal measurements to ensure physical relevance.

Indoor measurement methods

Indoor testing offers a controlled and reproducible complement to outdoor and theoretical PDRC assessment by replacing the sky with an artificial thermal sink under well-defined boundary conditions. A wide range of indoor platforms has been developed, spanning thermoelectric stages,[60] climatic chambers,[43] liquid-nitrogen (LN_2)-based cryogenic sinks,[36,61] and water-cooled or cryocooler-based systems[62] (see Table S4). More advanced configurations integrate solar simulators to enable combined daytime-nighttime characterization[63,64] (Figure 2).

Temperature-controlled stages and thermoelectric platforms allow direct measurement of net cooling power and temperature drop under fixed ambient temperature and humidity[60] but

Please cite this article in press as: Werlé et al., Performance assessment methods and metrics for passive daytime radiative cooling materials, Cell Reports Physical Science (2026), https://doi.org/10.1016/j.xcrp.2026.103225

CellPress
OPEN ACCESS

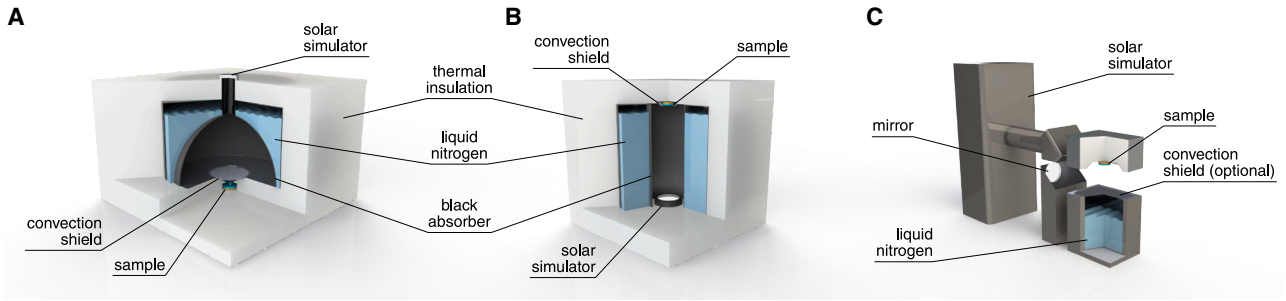

Figure 2. Representative indoor PDRC characterization setups with cryogenic heat sinks

(A) Dome configuration, where a liquid-nitrogen-cooled aluminum dome approximates a hemispherical sky, combined with a solar simulator and an IR-transparent convection shield.[65]

(B) Cylindrical configuration, in which the sample is placed at one end of a tubular heat sink and is illuminated from below by a solar simulator.[64]

(C) Reflected-illumination configuration, where the sample faces downward toward a convection-shielded LN_2 reservoir and solar radiation is redirected using a mirror.[63]

require careful treatment of IR wall reflections, sensor drift, and enclosure emissivity.

A key strength of indoor testing is repeatability: even if a given platform does not reproduce a realistic sky spectrum, it typically does so in a stable and predictable manner, enabling objective, condition-matched comparisons between materials. This is particularly valuable for rapid iteration, industrial screening, and model validation, where waiting for specific outdoor conditions is impractical. However, the extreme coldness of common cryogenic sinks (LN_2, $\sim$ 77 K) and the non-atmospheric spectral emissivity of internal chamber walls can significantly bias apparent cooling relative to clear-sky outdoor conditions (effective sky temperatures $\geq$ 200 K), limiting quantitative one-to-one comparison with outdoor FoMs.

Several test chambers further introduce pressure or gas-composition control, enabling direct quantification of parasitic conductive and convective heat fluxes.[66–68] Such platforms are particularly valuable for validating thermal models and deconvolving radiative from non-radiative losses, although they are not intended to reproduce realistic sky emissivity. Hybrid systems incorporating IR spectral filters, tunable dome temperatures, or adjustable view factors partially bridge this gap and allow discrimination between selective and broadband emitters under controlled conditions.[65] At larger scales, indoor water-cooled or thermosiphon-based setups enable panel-level testing and integration studies but similarly sacrifice spectral realism.[62]

For meaningful use and inter-laboratory comparability, key parameters, including effective sink/sky temperature, spectral mismatch, view factor, enclosure emissivity, pressure/gas conditions, and solar-simulator spectrum and uniformity, should be reported. Dome-type configurations are attractive because they naturally enforce a hemispherical view factor between the sample and the modeled sink, reducing sensitivity to sample-sink distance and simplifying interpretation. More generally, the integration of a solar simulator is advantageous for assessing daytime operation, and temperature and humidity control improves repeatability.

Indoor tests also obviate the need for strictly parallel measurements: because boundary conditions are controlled, multiple FoMs and multiple samples can be tested sequentially with high confidence that conditions are identical, which is often impossible outdoors. Accordingly, indoor data are best used comparatively to rank materials, isolate mechanisms, and validate models.

Nevertheless, they should be complemented by outdoor experiments and numerical modeling to ensure physical relevance beyond idealized conditions. In this combined framework, indoor testing provides a powerful tool for reproducible, cross-laboratory assessment of RC performance (see Table S4).

SUMMARY AND OUTLOOK

Given the continuous development of PDRC materials, establishing standardized performance assessment methods remains a major challenge (see Table S5). Most studies in the literature focus on two key indicators: the maximum sub-ambient temperature drop and the net cooling power at ambient temperature, ideally to be tested simultaneously. However, these metrics are sensitive to environmental conditions as well as test configuration, requiring clear reporting of boundary conditions, instrumentation, and data-processing assumptions. While numerical models using standard atmospheric data can support approximate comparisons, standardized indoor and outdoor test methods against reference benchmarks coupled with well-documented simulations are essential for reliable evaluation.

The following checklist summarizes the parameters recommended for reporting PDRC performance characterization.

Sample properties:

- Coating thickness and composition (or multilayer stack description), including the material, mass, and thickness of the substrate.
- Solar reflectance measured over a wavelength range covering at least the range 0.3–2.5 μm, using an absolute reflectance standard and averaging over at least three independent repeat measurements. Measurements should account for different in-plane sample orientations and include checks for detector switching wavelengths to ensure consistency.

- If compatible with the substrate composition, integrated transmittance in the same spectral range should also be reported to confirm the reflectance measurement and allow more precise determination of solar absorptance.
- Spectrally resolved IR emissivity (hemispherical, otherwise directional with the measurement geometry stated) over 3–30 μm, averaged over at least three independent repeat measurements and, where relevant, different in-plane orientations.
- When relevant for non-horizontal installations (e.g., targeting building façade applications), angle-resolved emissivity (or a directional emissivity integrated over the sky window) should be reported.
- When available, thermo-physical properties (e.g., thermal conductivity/diffusivity and contact-resistance considerations) should be provided, as measured by a suitable technique (e.g., laser-flash method).

PDRC performance:

- Maximum temperature drop and net cooling power at ambient temperature, with a clear definition of "ambient" and a description of how it is measured.
- When feasible, measure temperature drop and cooling power simultaneously using identical sample assemblies.
- Include both daytime and nighttime data, which provide a relevant consistency check and are useful to decouple cooling performance from the solar reflectivity of the sample.
- Perform the same measurements on standardized reference surfaces (e.g., reproducible DIY or industrial reference samples)[11,42,43] to provide a common baseline for cross-study comparisons.
- If aging is evaluated, adopt established procedures[24,69] with clear reporting of exposure conditions and test duration.
- Model, uncertainty, placement, and attachment method of sample temperature sensors (including how thermal contact is ensured and whether multiple points are monitored).
- Substrate and mounting details (material, thickness, mass, and adhesion method)
- Description of the thermal insulation of the sample holder, including properties and dimensions of the insulating materials used.
- Optical characterization of any holder covers or shields (e.g., Tyvek over aluminum foil) and, if used, of convection shields (e.g., PE films).
- Expanded uncertainty of reported outdoor performance metrics, including contributions from environmental sensors and geometric factors
- For small samples or limited insulation, estimating the non-radiative heat-transfer coefficient is recommended.[38,39]

Outdoor experimental conditions:

- Suitable testing period (ideally between 2 and 7 days), including representative clear-sky hours with high solar irradiance (typically 800–1,000 W m^{-2}) and preferably low wind (e.g., <2 m s^{-1}).
- Time, date, location, and altitude of the test site, to support atmospheric modeling and independent reproducibility.
- Sample orientation/tilt and tracking strategy (if any) should be avoided for simplicity or reported relative to solar noon or local horizon.
- Sky view factor and description of nearby obstacles and surroundings.
- Ambient temperature, humidity, and wind speed measured near the samples (properly shielded and at an appropriate height from the ground). If air-sealed boxes are used, additionally report temperature and humidity inside the enclosure.
- Total solar irradiance (instrument type, calibration/uncertainty, and measurement geometry).
- Downwelling long-wave radiation and/or effective sky temperature during the experiment (instrument type and field of view).

Indoor experimental conditions:

- Sample size and view factor between the sample and the cold sink (e.g., 2π for an ideal hemispherical dome; geometry-dependent otherwise).
- Temperatures of the cold sink, chamber walls, and the ambient environment surrounding the sample.
- Model and specifications of the equipment used, including solar simulators (spectral match and uniformity), airflow control, and pressure or gas-composition regulation (if present).
- Spectral properties (transmittance, reflectance, and absorbance) of optical elements (e.g., mirrors, filters, or windows) incorporated into the setup.
- Repeatability tests accounting for the thermal inertia of the platform and an expanded uncertainty estimate for the reported FoMs.

Numerical methods:

- Model type: scalar (broadband hemispherical properties) or, preferably, spectral and/or spectral directional.
- Provenance of atmospheric data: measurements, reanalysis databases (e.g., ECMWF ERA5[70]), or typical meteorological year files.
- Sky model/long-wave spectra (e.g., PSG,[53] MODTRAN,[52] TRNSYS,[71] RRTM_LW,[54,72] or empirical correlations[50,73]) and, if using transmittance-based approaches, any stratification-aware correction assumptions.[51]
- Solar spectrum source used for solar-weighted reflectance, reported explicitly. For comparability, report AM1.5G (e.g., ASTM G173/NREL tabulation).[17] For heat-gain relevance under typical horizontal outdoor illumination, additionally report AM1GH following Levinson et al.[18]
- Cloud model if used along with assumptions on clouds (e.g., cloud fraction/altitude/phase).
- Convection correlations, if used.
- Thermal flux assumption and boundary conditions assumed around the sample.
- Numerical scheme and coupling strategy for solving the heat balance.

Please cite this article in press as: Werlé et al., Performance assessment methods and metrics for passive daytime radiative cooling materials, Cell Reports Physical Science (2026), https://doi.org/10.1016/j.xcrp.2026.103225

The scientific community working on PDRC is encouraged to prioritize robust, well-documented protocols and benchmarking rather than focusing solely on peak performance values. Poorly reported conditions and non-representative protocols can create apparent outliers, hinder cross-laboratory comparisons, and ultimately undermine confidence in PDRC technologies among industrial and governmental stakeholders. Using coupled FoMs (e.g., reporting both cooling power and temperature drop) together with reference samples and transparent modeling is a practical path to reducing location-specific biases and improving comparability.

Finally, this checklist is not exhaustive. It focuses on UV-Vis-NIR-opaque PDRC coatings or solid reflectors with quasi-static optical properties. Other material classes—including textiles, semi-transparent/window concepts, and stimuli-responsive systems (e.g., phase-change, thermochromic, or photoluminescent materials)—may require additional, class-specific characterization protocols. For example, stimuli-responsive materials require state-resolved, temperature-controlled spectral measurements across operating states, while photoluminescent coatings may require optical filtering or radiometric methods to separate emitted from reflected light.

While application-specific FoMs may be required in some cases, the proposed framework provides a practical basis for standardized, comparable, and reproducible PDRC performance evaluation across research and industry. Looking ahead, coordinated round-robin inter-laboratory campaigns and openly shared reference datasets will be essential to convert these recommendations into broadly adopted standards and to accelerate the translation of PDRC materials from laboratory demonstrations to deployable technologies. Establishing shared protocols and reference baselines will also enable meaningful cross-study meta-analyses and more defensible comparisons across climates and test setups.

ACKNOWLEDGMENTS

The project 21GRD03 PaRaMetriC received funding from the European Partnership on Metrology, co-financed by the European Union's Horizon Europe Research and Innovation Programme and from the Participating States. J.W. would like to thank Alexis Guehennec for his contributions and assistance in realizing the 3D setup schemes.

AUTHOR CONTRIBUTIONS

Conceptualization, D.T., J.W., and L.P.; methodology, D.T., J.W., and L.P.; investigation, D.T., J.W., and L.P.; visualization, J.W.; supervision, L.P., C.E., M.-N.A., and M.V.; project administration, L.P., C.E., and M.-N.A.; writing – original draft, D.T.; writing – review & editing, J.W., L.P., C.E., M.-N.A., and M.V.

DECLARATION OF INTERESTS

The authors declare no competing interests.

DECLARATION OF GENERATIVE AI AND AI-ASSISTED TECHNOLOGIES IN THE WRITING PROCESS

During the preparation of this work, the authors used ChatGPT in order to improve grammar. After using this tool, the authors reviewed and edited the content as needed and take full responsibility for the content of the publication.

SUPPLEMENTAL INFORMATION

Supplemental information can be found online at https://doi.org/10.1016/j.xcrp.2026.103225.

REFERENCES

1. Copernicus Climate Change Service (C3S). Copernicus: 2025 Was the Third-Hottest Year on Record (2026). Web publication; accessed 2026-02-08. https://climate.copernicus.eu/copernicus-2025-was-third-hottest-year-record.
2. United Nations Environment Programme (2023). Global Cooling Watch 2023: Keeping it Chill: How to Meet Cooling Demands while Cutting Emissions. https://www.unep.org/resources/global-cooling-watch-2023.
3. Yin, X., Yang, R., Tan, G., and Fan, S. (2020). Terrestrial radiative cooling: Using the cold universe as a renewable and sustainable energy source. Science *370*, 786–791. https://doi.org/10.1126/science.abb0971.
4. Raman, A.P., Anoma, M.A., Zhu, L., Rephaeli, E., and Fan, S. (2014). Passive radiative cooling below ambient air temperature under direct sunlight. Nature *515*, 540–544. https://doi.org/10.1038/nature13883.
5. Carlosena, L., Ruiz-Pardo, Á., Feng, J., Irulegi, O., Hernández-Minguillón, R.J., and Santamouris, M. (2020). On the energy potential of daytime radiative cooling for urban heat island mitigation. Sol. Energy *208*, 430–444. https://doi.org/10.1016/j.solener.2020.08.015.
6. Lee, M., Kim, G., Jung, Y., Pyun, K.R., Lee, J., Kim, B.-W., and Ko, S.H. (2023). Photonic structures in radiative cooling. Light Sci. Appl. *12*, 134. https://doi.org/10.1038/s41377-023-01119-0.
7. Yu, X., Chan, J., and Chen, C. (2021). Review of radiative cooling materials: Performance evaluation and design approaches. Nano Energy *88*, 106259. https://doi.org/10.1016/j.nanoen.2021.106259.
8. Aili, A., Zhao, D., Lu, J., Zhai, Y., Yin, X., Tan, G., and Yang, R. (2019). A kW-scale, 24-hour continuously operational, radiative sky cooling system: Experimental demonstration and predictive modeling. Energy Convers. Manag. *186*, 586–596. https://doi.org/10.1016/j.enconman.2019.03.006.
9. Zhao, D., Aili, A., Yin, X., Tan, G., and Yang, R. (2019). Roof-integrated radiative air-cooling system to achieve cooler attic for building energy saving. Energy Build. *203*, 109453. https://doi.org/10.1016/j.enbuild.2019.109453.
10. Bu, K., Huang, X., Li, X., and Bao, H. (2023). Consistent assessment of the cooling performance of radiative cooling materials. Adv. Funct. Mater. *33*, 2307191. https://doi.org/10.1002/adfm.202307191.
11. Adibekyan, A., Schumacher, J., Pattelli, L., Manara, J., Meriç, S., Bazkir, Ö., Cucchi, C., Sprengard, C., Pérez, G., Campos, J., et al. (2025). Emissivity and reflectivity measurements for passive radiative cooling technologies. Int. J. Thermophys. *46*, 66. https://doi.org/10.1007/s10765-025-03532-6.
12. Gentle, A.R., and Smith, G.B. (2016). Is enhanced radiative cooling of solar cell modules worth pursuing? Sol. Energy Mater. Sol. Cell. *150*, 39–42. https://doi.org/10.1016/j.solmat.2016.01.039.
13. Zhou, L., Yin, X., and Gan, Q. (2023). Best practices for radiative cooling. Nat. Sustain. *6*, 1030–1032. https://doi.org/10.1038/s41893-023-01170-0.
14. He, Y., Lu, B., Zhi, Y., Zhang, H., Yu, H., Lu, Y., Wan, R., Sun, L., Yang, H., Zhou, Q., et al. (2025). Radiative property tests of cooling coatings: A round robin campaign. Energy Build. *345*, 116073. https://doi.org/10.1016/j.enbuild.2025.116073.
15. Valenta, J., Fucikova, A., Greben, M., Khan, H.S., Paolini, R., Garshasbi, S., and Santamouris, M. (2024). Radiometric characterization of daytime luminescent materials directly under the solar illumination. AIP Adv. *14*, 105113. https://doi.org/10.1063/5.0235354.

Please cite this article in press as: Werlé et al., Performance assessment methods and metrics for passive daytime radiative cooling materials, Cell Reports Physical Science (2026), https://doi.org/10.1016/j.xcrp.2026.103225

16. Wang, Z., Pian, S., and Ma, Y. (2025). Characterization of radiative cooling materials. Nat. Protoc. https://doi.org/10.1038/s41596-025-01273-2.

17. National Renewable Energy Laboratory (NREL) (2026). Reference Air Mass 1.5 Solar Spectral Irradiance (ASTM G-173). https://www.nrel.gov/grid/solar-resource/spectra-am1.5. https://www.nrel.gov/grid/solar-resource/spectra-am1.5 standard terrestrial solar spectral irradiance, direct normal and global tilt spectra for AM1.5.

18. Levinson, R., Akbari, H., and Berdahl, P. (2010). Measuring solar reflectance–Part I: Defining a metric that accurately predicts solar heat gain. Sol. Energy *84*, 1717–1744. https://doi.org/10.1016/j.solener.2010.04.018.

19. Granqvist, C.G., and Hjortsberg, A. (1981). Radiative cooling to low temperatures: General considerations and application to selectively emitting sio films. J. Appl. Phys. *52*, 4205–4220. https://doi.org/10.1063/1.329270.

20. Akbari, H., Levinson, R., and Berdahl, P. (1996). ASTM standards for measuring solar reflectance and infrared emittance of construction materials and comparing their steady-state surface temperatures. In 1996 ACEEE Summer Study on Energy Efficiency in Buildings (American Council for an Energy-Efficient Economy).

21. Fabiani, C., Muscio, A., and Pisello, A.L. (2025). Introducing the enhanced solar reflectance index (sri*) for comprehensive evaluation of spectrally selective cool materials in real-world scenarios. Sustain. Energy Technol. Assessments *81*, 104415. https://doi.org/10.1016/j.seta.2025.104415.

22. Li, X., Peoples, J., Huang, Z., Zhao, Z., Qiu, J., and Ruan, X. (2020). Full daytime sub-ambient radiative cooling in commercial-like paints with high figure of merit. Cell Rep. Phys. Sci. *1*, 100221. https://doi.org/10.1016/j.xcrp.2020.100221.

23. Muscio, A. (2018). The solar reflectance index as a tool to forecast the heat released to the urban environment: Potentiality and assessment issues. Climate *6*, 12. https://doi.org/10.3390/cli6010012.

24. Paolini, R., Terraneo, G., Ferrari, C., Sleiman, M., Muscio, A., Metrangolo, P., Poli, T., Destaillats, H., Zinzi, M., and Levinson, R. (2020). Effects of soiling and weathering on the albedo of building envelope materials: Lessons learned from natural exposure in two European cities and tuning of a laboratory simulation practice. Sol. Energy Mater. Sol. Cell. *205*, 110264. https://doi.org/10.1016/j.solmat.2019.110264.

25. Sleiman, M., Ban-Weiss, G., Gilbert, H.E., François, D., Berdahl, P., Kirchstetter, T.W., Destaillats, H., and Levinson, R. (2011). Soiling of building envelope surfaces and its effect on solar reflectance – Part I: Analysis of roofing product databases. Sol. Energy Mater. Sol. Cell. *95*, 3385–3399. https://doi.org/10.1016/j.solmat.2011.08.002.

26. Sleiman, M., Kirchstetter, T.W., Berdahl, P., Gilbert, H.E., Quelen, S., Marlot, L., Preble, C.V., Chen, S., Montalbano, A., Rosseler, O., et al. (2014). Soiling of building envelope surfaces and its effect on solar reflectance – Part II: Development of an accelerated aging method for roofing materials. Sol. Energy Mater. Sol. Cell. *122*, 271–281. https://doi.org/10.1016/j.solmat.2013.11.028.

27. Sleiman, M., Chen, S., Gilbert, H.E., Kirchstetter, T.W., Berdahl, P., Bibian, E., Bruckman, L.S., Cremona, D., French, R.H., Gordon, D.A., et al. (2015). Soiling of building envelope surfaces and its effect on solar reflectance – Part III: Interlaboratory study of an accelerated aging method for roofing materials. Sol. Energy Mater. Sol. Cell. *143*, 581–590. https://doi.org/10.1016/j.solmat.2015.07.031.

28. Mandal, J., Anand, J., Mandal, S., Brewer, J., Ramachandran, A., and Raman, A.P. (2024). Radiative cooling and thermoregulation in the Earth's glow. Cell Rep. Phys. Sci. *5*, 102065. https://doi.org/10.1016/j.xcrp.2024.102065.

29. Leroy, A., Bhatia, B., Kelsall, C.C., Castillejo-Cuberos, A., Di Capua H, M., Zhao, L., Zhang, L., Guzman, A.M., and Wang, E.N. (2019). High-performance subambient radiative cooling enabled by optically selective and thermally insulating polyethylene aerogel. Sci. Adv. *5*, eaat9480. https://doi.org/10.1126/sciadv.aat9480.

30. Choi, M., Seo, J., Yoon, S., Nam, Y., Lee, J., and Lee, B.J. (2022). All-day radiative cooling using a grating-patterned PDMS film emitter. Appl. Therm. Eng. *214*, 118771. https://doi.org/10.1016/j.applthermaleng.2022.118771.

31. Goldstein, E.A., Raman, A.P., and Fan, S. (2017). Sub-ambient non-evaporative fluid cooling with the sky. Nat. Energy *2*, 17143. https://doi.org/10.1038/nenergy.2017.143.

32. Lopardo, G., Bertiglia, F., Braccialarghe, G., Florio, M., Girard, F., Giraudi, D., Santoro, F., and Pattelli, L. (2026). Metrological setup for accurate determination of passive radiative cooling power. Appl. Therm. Eng. *292*, 130363. https://doi.org/10.1016/j.applthermaleng.2026.130363.

33. Aili, A., Yin, X., and Yang, R. (2021). Global radiative sky cooling potential adjusted for population density and cooling demand. Atmosphere *12*, 1379. https://doi.org/10.3390/atmos12111379.

34. Hu, M., Zhao, B., Suhendri, Cao, J., Cao, J., Wang, Q., Riffat, S., Su, Y., and Pei, G. (2022). Quantitative characterization of the effect of inclination angle on flat-plate radiative cooling performance in buildings. J. Build. Eng. *59*, 105124. https://doi.org/10.1016/j.jobe.2022.105124.

35. Zhao, B., Ao, X., Chen, N., Xuan, Q., Hu, M., and Pei, G. (2019). General strategy of passive sub-ambient daytime radiative cooling. Sol. Energy Mater. Sol. Cell. *199*, 108–113. https://doi.org/10.1016/j.solmat.2019.04.028.

36. Zhou, L., Song, H., Liang, J., Singer, M., Zhou, M., Stegenburgs, E., Zhang, N., Xu, C., Ng, T., Yu, Z., et al. (2019). A polydimethylsiloxane-coated metal structure for all-day radiative cooling. Nat. Sustain. *2*, 718–724. https://doi.org/10.1038/s41893-019-0348-5.

37. Zhang, J., Yuan, J., Liu, J., Zhou, Z., Sui, J., Xing, J., and Zuo, J. (2021). Cover shields for sub-ambient radiative cooling: A literature review. Renew. Sustain. Energy Rev. *143*, 110959. https://doi.org/10.1016/j.rser.2021.110959.

38. Fan, F., Xu, D., Zhu, Y., Tan, G., and Zhao, D. (2023). A simple, accurate, and universal method for characterizing and comparing radiative cooling materials and devices. Int. J. Heat Mass Tran. *200*, 123494. https://doi.org/10.1016/j.ijheatmasstransfer.2022.123494.

39. Catalanotti, S., Cuomo, V., Piro, G., Ruggi, D., Silvestrini, V., and Troise, G. (1975). The radiative cooling of selective surfaces. Sol. Energy *17*, 83–89. https://doi.org/10.1016/0038-092X(75)90062-6.

40. Lio, G.E., Werlé, J., Arduini, M., Wiersma, D.S., Manara, J., and Pattelli, L. (2024). Radiative cooling potential of a water-based paint formulation under realistic application conditions. ACS Appl. Opt. Mater. *2*, 2459–2468. https://doi.org/10.1021/acsaom.4c00099.

41. Werlé, J., Concas, R., Pini, E., Wiersma, D.S., Pattelli, L., and Lio, G.E. (2025). Open-hardware platform for synchronous performance testing of multiple passive radiative cooling materials. Cell Rep. Phys. Sci. *6*, 102688. https://doi.org/10.1016/j.xcrp.2025.102688.

42. Huang, X., Mandal, J., and Raman, A.P. (2021). Do-it-yourself radiative cooler as a radiative cooling standard. J. Photonics Energy *12*, 012112. https://doi.org/10.1117/1.JPE.12.012112.

43. Chiatti, C., Marchini, F., Fabiani, C., Kousis, I., Carlosena, L., and Pisello, A.L. (2024). Harnessing the potential of radiative cooling for the built environment: A new comprehensive protocol for materials' characterization. Sol. Energy Mater. Sol. Cell. *277*, 113074. https://doi.org/10.1016/j.solmat.2024.113074.

44. Hu, J., Xia, X., and Xia, Z. (2025). The impact of test device on the evaluation cooling effect of radiation-cooling materials. Materials *18*, 1512. https://doi.org/10.3390/ma18071512.

45. Haddouche, M.R., Martorell, I., Solé, C., Castell, A., and Medrano, M. (2026). Experimental investigation of parameters influencing test box and material behavior in daytime radiative cooling measurements. Heat Trans. *55*, 18–30. https://doi.org/10.1002/htj.23362.

46. Sui, C., and Hsu, P.-C. (2024). Standardizing the thermodynamic definition of daytime subambient radiative cooling. ACS Energy Lett. *9*, 2997–3000. https://doi.org/10.1021/acsenergylett.4c00909.

Please cite this article in press as: Werlé et al., Performance assessment methods and metrics for passive daytime radiative cooling materials, Cell Reports Physical Science (2026), https://doi.org/10.1016/j.xcrp.2026.103225

47. Feng, J., and Santamouris, M. (2019). Numerical techniques for electromagnetic simulation of daytime radiative cooling: A review. AIMS Mater. Sci. *6*, 1049–1064. https://doi.org/10.3934/matersci.2019.6.1049.

48. Jin, Y., and Kats, M. (2025). A gradient atmospheric model reveals enhanced radiative cooling potential and demonstrates the advantages of broadband emitters. Laser Photon. Rev. *19*, e00371. https://doi.org/10.1002/lpor.202500371.

49. Lee, D., Kwon, S., and Kim, M. (2023). ViBA Rad: Visualization and basic analysis tools for radiative cooling. SoftwareX *24*, 101562. https://doi.org/10.1016/j.softx.2023.101562.

50. Wong, R.Y.M., Tso, C.Y., Jeong, S.Y., Fu, S.C., and Chao, C.Y.H. (2023). Critical sky temperatures for passive radiative cooling. Renew. Energy *211*, 214–226. https://doi.org/10.1016/j.renene.2023.04.142.

51. Mandal, J., Huang, X., and Raman, A.P. (2021). Accurately quantifying clear-sky radiative cooling potentials: A temperature correction to the transmittance-based approximation. Atmosphere *12*, 1195. https://doi.org/10.3390/atmos12091195.

52. Berk, A., Conforti, P., Kennett, R., Perkins, T., Hawes, F., and van den Bosch, J. (2014). MODTRAN6: A major upgrade of the MODTRAN® radiative transfer code. In *Algorithms and Technologies for Multispectral, Hyperspectral, and Ultraspectral Imagery XX* vol. 9088 of *Proceedings of SPIE* (SPIE). https://doi.org/10.1117/12.2050433.

53. Villanueva, G.L., Smith, M.D., Protopapa, S., Faggi, S., and Mandell, A.M. (2018). Planetary Spectrum Generator: an accurate online radiative transfer suite for atmospheres, comets, small bodies and exoplanets. J. Quant. Spectrosc. Radiat. Transf. *217*, 86–104. https://doi.org/10.1016/j.jqsrt.2018.05.023.

54. Pattelli, L., and Belotti, C. (2024). PASTICHE: The PaRaMetriC Atmospheric Spectral Tool for Irradiance Calculation using Hourly ERA5 data. https://github.com/21grd03-parametric/pastichesoftware.

55. Yu, X., and Chen, C. (2021). Coupling spectral-dependent radiative cooling with building energy simulation. Build. Environ. *197*, 107841. https://doi.org/10.1016/j.buildenv.2021.107841.

56. Chen, H., Wei, J., Liu, X., Liu, J., and Wang, C. (2025). Assessing radiative cooling power considering the cloud effects. Appl. Therm. Eng. *278*, 127192. https://doi.org/10.1016/j.applthermaleng.2025.127192.

57. Seo, J., Choi, M., Yoon, S., and Lee, B.J. (2023). Climate-dependent optimization of radiative cooling structures for year-round cold energy harvesting. Renew. Energy *217*, 119166. https://doi.org/10.1016/j.renene.2023.119166.

58. Bu, F., Yan, D., Tan, G., Sun, H., and An, J. (2022). Systematically incorporating spectrum-selective radiative cooling into building performance simulation: Numerical integration method and experimental validation. Appl. Energy *312*, 118733. https://doi.org/10.1016/j.apenergy.2022.118733.

59. Forte, D., Belotti, C., Pattelli, L., Morciano, M., Chiavazzo, E., Asinari, P., and Fasano, M. (2025). Modeling of daytime radiative cooling enhanced vapor-compression refrigeration systems. Energy *340*, 139101. https://doi.org/10.1016/j.energy.2025.139101.

60. Wong, R.Y.M., Tso, C.Y., and Chao, C.Y.H. (2021). Corrected radiative cooling power measured by equivalent dissipative thermal reservoir method. Int. J. Heat Mass Tran. *174*, 121341. https://doi.org/10.1016/j.ijheatmasstransfer.2021.121341.

61. Tam, H.T.T., Toma, M., Okamoto, T., Hidaka, M., Fujii, K., Kuwana, Y., and Kajikawa, K. (2023). Weatherable, solvent-soluble, paintable and transparent fluoropolymers for daytime radiative cooling. Int. J. Therm. Sci. *184*, 107959. https://doi.org/10.1016/j.ijthermalsci.2022.107959.

62. Zhao, D., Martini, C.E., Jiang, S., Ma, Y., Zhai, Y., Tan, G., Yin, X., and Yang, R. (2017). Development of a single-phase thermosiphon for cold collection and storage of radiative cooling. Appl. Energy *205*, 1260–1269. https://doi.org/10.1016/j.apenergy.2017.08.057.

63. Fang, H., Zhou, L., Xu, L., Dang, S., De Wolf, S., and Gan, Q. (2024). Radiative cooling for vertical solar panels. iScience *27*, 108806. https://doi.org/10.1016/j.isci.2024.108806.

64. Park, G., Roh, K., Kim, H., Khan, S., Lee, M., Kim, B.-W., and Kim, W. (2022). Universal experimental methods for evaluating the performance of radiative cooling materials. Adv. Mater. Technol. *7*, 2101205. https://doi.org/10.1002/admt.202101205.

65. Song, Q., Tran, T., Herrmann, K., Lauster, T., Breitenbach, M., and Retsch, M. (2022). A tailored indoor setup for reproducible passive daytime cooling characterization. Cell Rep. Phys. Sci. *3*, 100986. https://doi.org/10.1016/j.xcrp.2022.100986.

66. Swanger, A.M., Krenn, A., Youngquist, R., and Gibson, T.L. (2022). Development of a space irradiance simulator for advanced studies and materials research. IOP Conf. Ser. Mater. Sci. Eng. *1240*, 012006. https://doi.org/10.1088/1757-899X/1240/1/012006.

67. Banik, U., Meddeb, H., Berends, D., Reininghaus, N., Sergeev, O., Busch, L., Gehrke, K., Vehse, M., and Agert, C. (2024). Impact of parasitic heat fluxes on deep sub-ambient radiative coolers under variable pressure. Appl. Therm. Eng. *237*, 121655. https://doi.org/10.1016/j.applthermaleng.2023.121655.

68. Leroy, A., Bhatia, B., Sircar, J., and Wang, E.N. (2022). Thermal transport in solar-reflecting and infrared-transparent polyethylene aerogels. Int. J. Heat Mass Tran. *184*, 122307. https://doi.org/10.1016/j.ijheatmasstransfer.2021.122307.

69. ASTM International. Standard practice for laboratory soiling and weathering of roofing materials to simulate effects of natural exposure on solar reflectance and thermal emittance. ASTM D7897-18 (2018). Standard practice for laboratory soiling and weathering of roofing materials. https://doi.org/10.1520/D7897-18.

70. Hersbach, H., Bell, B., Berrisford, P., Hirahara, S., Horányi, A., Muñoz Sabater, J., Nicolas, J., Peubey, C., Radu, R., Schepers, D., et al. (2020). The ERA5 global reanalysis. Q. J. R. Meteorol. Soc. *146*, 1999–2049.

71. Solar Energy Laboratory (2017). University of Wisconsin–Madison. TRNSYS 18: A transient system simulation program. http://sel.me.wisc.edu/trnsyssoftwaremanual/documentation. http://sel.me.wisc.edu/trnsys.

72. Mlawer, E.J., Taubman, S.J., Brown, P.D., Iacono, M.J., and Clough, S.A. (1997). Radiative transfer for inhomogeneous atmospheres: Rrtm, a validated correlated-k model for the longwave. J. Geophys. Res. *102*, 16663–16682. https://doi.org/10.1029/97JD00237.

73. Evangelisti, L., Guattari, C., and Asdrubali, F. (2019). On the sky temperature models and their influence on buildings energy performance: A critical review. Energy Build. *183*, 607–625. https://doi.org/10.1016/j.enbuild.2018.11.037.